Journal Name

ARTICLE

Wide Band-gap Tuning in Sn-based Hybrid Perovskites through Cation Replacement: the $FA_{1-x}MA_xSnBr_3$ Mixed System

Received 00th January 20xx,
Accepted 00th January 20xx

DOI: 10.1039/x0xx00000x

www.rsc.org/

Chiara Ferrara,[a] Maddalena Patrini,[b] Ambra Pisanu,[a] Paolo Quadrelli,[a] Chiara Milanese,[a] Cristina Tealdi,[a] and Lorenzo Malavasi[a,*]

We report the synthesis and characterization of the first Sn-based mixed system, namely $FA_{1-x}MA_xSnBr_3$ ($0 \le x \le 1$), providing also the first study of the $FASnBr_3$ hybrid perovskite. The results indicate the formation of a continuous solid solution between the two end members with a huge modulation of the band-gap induced by the cation replacement. These results suggest the key role of protonated amines on the electronic structure in tin-based systems and a new and effective way of tuning the band-gap.

Introduction

Modulation of hybrid perovskite properties by means of protonated amine substitution is a very appealing and fascinating way of performing such tuning with the aim, for example, of extending and/or changing the absorption edge and improve materials stability.[1-9] In particular, mixed lead iodide systems based on methylammonium (MA) and formamidinium (FA) cations have attracted significant interest because: i) the larger FA cation leads to more symmetric perovskites with respect to $MAPbI_3$ (MAPI) phase (which is tetragonal at room temperature); ii) the smaller band-gap of $FAPbI_3$ (FAPI) allows the near-IR absorption, and iii) perovskites containing FA cation have an improved stability.[1-4]

On the other hand, another investigated substitution route is the Sn replacement for Pb in order to exploit the use of environmental-friendly hybrid perovskites.[8-15] Very recently, improved performance has been obtained for Sn-based perovskite solar cells, which suggests that a proper control of the active layer, in particular the limitation of the Sn^{2+} oxidation, may lead to usable devices.[16-20]

Tuning the hybrid perovskite properties by ion replacement makes a great difference, e.g. in the extension os such modulation, according to the ion considered. B-site or X-site ions replacement is highly efficient in terms, for example, of the absorption energy interval that can be modulated. For instance, Br for I substitution in most of the hybrid perovskites leads to an overall variation of the band-gap (E_g) close to 0.7 eV.[3] Sn for Pb substitution on the B-site may increase the energy interval up to 0.9 eV[9]. On the other hand, A-site cation substitution is significantly less effective in such absorption modulation, with an overall variation of the E_g lower than 0.1 eV when changing from MA to FA in Pb-based halide perovskites.[3] However, the replacement of different protonated amines in these systems is very attractive having a great impact on properties such as carrier lifetime, that is less influenced by B-site or X-site ion substitution. In order to explore a new and efficient way of modulating the photon absorption properties in environmental friendly hybrid perovskite, we undertook the investigation of FA/MA mixed systems in tin-based materials.

Most of the Sn-based organic-inorganic perovskites investigations centre on methylammonium cation and iodide anion, *i.e.* the $MASnI_3$ material, having a band-gap value around 1.2-1.3 eV and a tetragonal crystal structure.[20] Less extensive investigations are available regarding other protonated amines and/or halogens in Sn-based systems.

$MASnBr_3$, showing a cubic structure and a band-gap around 2.2 eV, has been recently reported in perovskite solar cells where the perovskite has been fabricated by means of vapour assisted methods in order to make it rich in Sn^{2+}.[22] Some attention has been also devoted to tin-based perovskites containing the FA cation ($FASnI_3$), with efficiencies around 5% and very long-term stability promoted by encapsulation of the absorber.[12,23]

Most of the problems of Sn-based hybrid perovskites relate to the proper control of the tin oxidation state. We already showed that reliable structural and optical performances require a strict control over this parameter.[8,9] In addition, in the actual literature, there are no reports about mixed A-cation compositions of tin perovskites as it has extensively reported for Pb-based materials.[3]

In order to start filling this gap, in the present paper we explored, for the first time, the synthesis and characterization of the $FA_{1-x}MA_xSnBr_3$ system by paying particular attention on the control of effective cation composition. Moreover, for the first time, it is reported the synthesis and the structural and optical characterization of the $FASnBr_3$ hybrid perovskite.

Experimental

Samples of general formula $FA_{1-x}MA_xSnBr_3$ (with nominal x=0, 0.05, 0.2, 0.3, 0.6, 0.8 and 1) were synthesized according to a general and original procedure we developed.[8,9] In a typical

[a] Department of Chemistry, University of Pavia, Viale Taramelli 16, 27100 Pavia, Italy.
[b] Department of Physics, University of Pavia, Via Bassi 6, 27100 Pavia, Italy.
† Footnotes relating to the title and/or authors should appear here.
Electronic Supplementary Information (ESI) available: Rietveld refinement data for $FASnBr_3$. See DOI: 10.1039/x0xx00000x

synthesis, a proper stoichiometric amount of Sn acetate is dissolved in an HBr excess under continuous mechanical stirring under nitrogen atmosphere. Hypophosphoric acid is added to the solution and inert atmosphere is maintained in the reaction environment in order to prevent Sn oxidation. Subsequently, the solution is heated to 100°C and the corresponding amines solutions (40%wt in water) are added in the stoichiometric amount to achieve the desired FA:MA ratio. The as obtained final solution is then cooled down to 46°C at 1°C/min, until the formation of a precipitate, that is immediately filtered and dried under vacuum overnight. All the reagents were purchased from Sigma Aldrich in pure form and were used without any further purification. The final products are handled and stored in a glove box with oxygen and water contents lower than 1 ppm. The crystal structure of the samples has been characterized at room temperature. Cu-radiation laboratory X-ray Powder Diffraction (XRD) data were acquired with a Bruker D5005 diffractometer by using a Bruker dome sealed in the glove box avoiding air exposure. High resolution synchrotron data for $FASnBr_3$ have been collected on ID22 (ESRF) in transmission mode with λ=0.176 Å with the sample filled into a quartz capillary. Diffraction data have been refined according to the Rietveld method to derive cell parameters and volume with the use of FullProf package.[24] The optical diffuse reflectance spectra of the different perovskites were measured from 0.8 to 4.5 eV (250-1500 nm, with steps of 1 nm) by a Varian Cary 6000i instrument equipped with an integrating sphere. For this kind of measurements, polycrystalline powders were loaded in 1 mm optical path cuvettes made of special optical glass (Hellma). ^{1}H solid state NMR room temperature measurements have been performed on a 9.4 T (^{1}H = 400.16 MHz) Bruker Avance III with the use of TopSpin 3.1 software; spectra have been collected with a 4 mm MAS probe under 8 kHz spinning conditions. ^{1}H quantitative one pulse experiments have been collected with a pulse length of 4.65 μs, recycle delay of 120 s and 16 scans. Pulse lengths and recycle delay have been carefully calibrated before the acquisition of the final spectra to ensure the full relaxation of the magnetization and fulfill the conditions for the quantitative data acquisition. Chemical shifts are referred to TMS using adamantane as secondary standard. The analysis of the obtained data has been performed with the use of DMFit program.[25] All the manipulations and measurements of the samples have been carried out under inert conditions in order to avoid tin oxidation.

Results and Discussion

As mentioned above, in order to provide the most reliable and accurate correlation between physical properties and composition, the prepared samples have been investigated by solid state ^{1}H NMR spectroscopy in order to determine their *real* FA:MA content. Such approach has been already shown to be effective in estimating the A-site composition.[26] ^{1}H MAS spectra for the whole $FA_{1-x}MA_xSnBr_3$ series, together with the corresponding attribution and the best fit for the two end members, are reported in Figure 1.

The spectrum of the $FASnBr_3$ composition presents two peaks at 9.81 ppm and 9.02 ppm with relative ratio 4:1 and these signals can be attributed to the $–NH_2$ and –CH protons, respectively. Similar chemical shifts have been observed for the NMR signal (liquid) of the $HC(NH_2)_2I$ and FAI precursors used for the synthesis of FAPI.[27,28] Similarly, the attribution for the $MASnBr_3$ composition has been made considering the presence of the two resonances at 7.73 and 4.72 ppm with ~ 1:1 ratio. These two signals have been previously correlated, respectively, to the $–NH_3^+$ and $– CH_3$ protons for the series $MAPbX_3$ (X = I, Br, Cl).[29] The signals of the two MA and FA species are only partially overlapped and under the experimental MAS speed (8 kHz) the observed lines are sufficiently sharp. The acquisition parameters (pulse length and recovery delay) have been optimized to obtain fully relaxed signals and allows for the quantitative analysis of the data. The ratio of peak integrals of the characteristic MA and FA cation resonances were calculated for each spectrum to determine the stoichiometry of the compound. It was found that the actual FA:MA stoichiometries, determined by NMR, were in good agreement with the nominal compositions (*i.e.*, those used in the preparation of the samples) within an estimated standard deviation of about 5%.

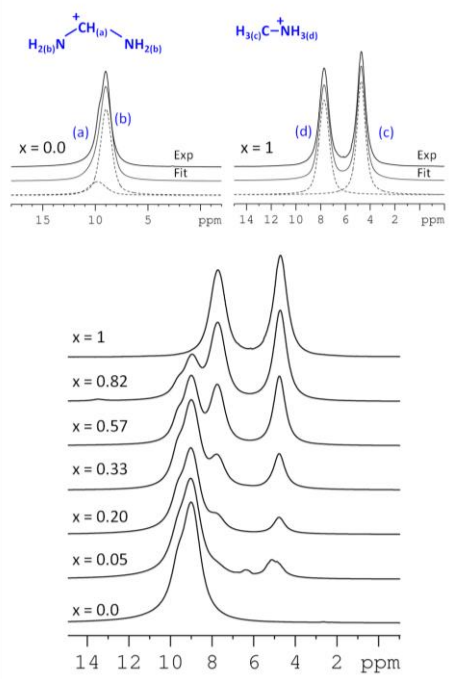

Figure 1. Solid state NMR spectra of the $FA_{1-x}MA_xSnBr_3$ solid solution. Top panel of the Figure: NMR spectra of $FASnBr_3$ (left) and $MASnBr_3$ (right) where dashed lines represent fit contributions and the solid light line the overall best-fit to the experimental spectra.

From this point on, we will refer to the sample by quoting the "real" stoichiometries found with NMR measurements.

The prepared samples have been characterized by means of laboratory X-ray diffraction (XRD). Figure 2 reports the patterns for the $FA_{1-x}MA_xSnBr_3$ series in the 10-70° range.

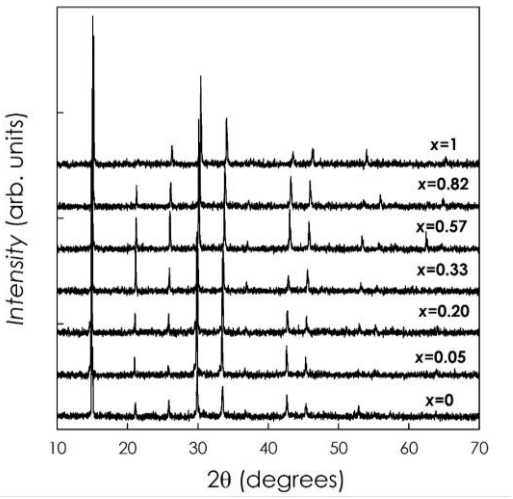

Figure 2. XRD patterns for the samples of the $FA_{1-x}MA_xSnBr_3$ system. Patterns are vertically shifted to clarify viewing

The crystal structure of $MASnBr_3$ has been object of a detailed structural analysis and has been indexed with a cubic lattice (space group, s.g., *Pm*-3*m*).[30] On the other hand, $FASnBr_3$ has never been reported in the current literature. From the comparison of the laboratory XRD patterns reported in Figure 2, we could observe that all the samples of the $FA_{1-x}MA_xSnBr_3$ system present analogous reflections in the diffraction patterns, which are also free from detectable impurities. For the $FASnBr_3$ sample, due to the lack of previous structural studies, we collected a high-resolution synchrotron diffraction pattern (λ=0.176 Å). The Rietveld refinement of this pattern using, as starting model, the cubic *Pm*-3*m* symmetry as for $MASnBr_3$, is reported in Figure 3.

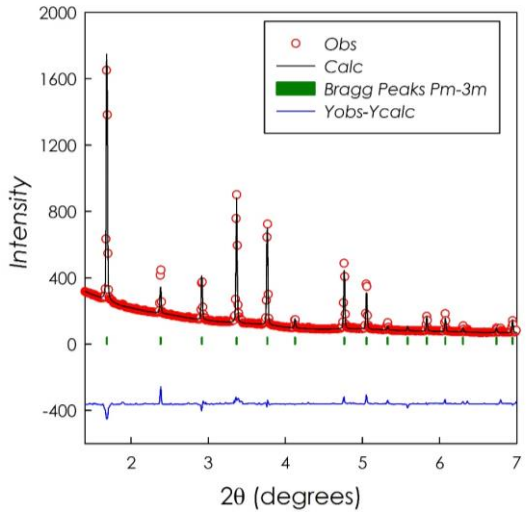

Figure 3. Rietveld refinement of synchrotron data (λ=0.176 Å) for $FASnBr_3$.

The good agreement of the refinement (R_{wp}=7.94, χ^2=1.65) suggests that the cubic lattice of $MASnBr_3$ is retained along with the MA/FA substitution on the perovskite A-lattice for the whole *x*-range.

The trend of the cubic lattice parameter, *a*, as a function of *x*, determined from the patterns of the $FA_{1-x}MA_xSnBr_3$ system shown in Figure 2, is reported in Figure 4.

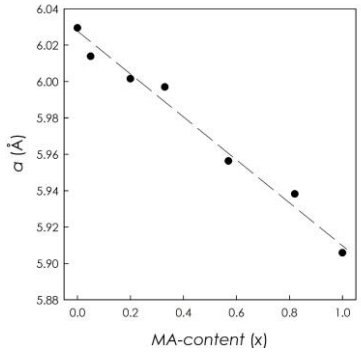

Figure 4. a) Cubic lattice parameter and b) cell volume for the $FA_{1-x}MA_xSnBr_3$ system as a function of x.

As can be appreciated from Figure 4, a linear decrease of the cubic *a* lattice parameter is found along with the increase of the amount of the smaller MA cation in the system (MA r_{eff} = 217 pm and FA r_{eff} = 253 pm).[6] This behaviour is consistent with the Vegard's law of solid solution formation, along with the same symmetry for the two end-members of the series (i.e., $FASnBr_3$ and $MASnBr_3$), and indicates the formation of a continuous solid solution in the $FA_{1-x}MA_xSnBr_3$ system, in analogy with the previous observation on $FA_{1-x}MA_xPbI_3$.[6] As a matter of fact, the structural results reported here are the first evidence of the existence of a solid solution in a tin-based hybrid perovskite. The search for solid-solution in this class of materials is of significant importance since the modulation of *x* may allow a corresponding optical properties modulation, as shown later in the text.

Optical measurements have been carried out on the $FA_{1-x}MA_xSnBr_3$ samples in order to define the band-gap values as a function of cation stoichiometry. Figures 5a and 5b report the vis-NIR diffuse reflectance spectra (R) and the trend of band-gap energy as a function of *x*, respectively. The E_g values have been obtained from the extrapolation of the linear part of $[F(R)\ h\nu]^2$ where F(R) is the Kubelka-Munk function $F(R) = (1-R)^2/2R$.[31, 32]

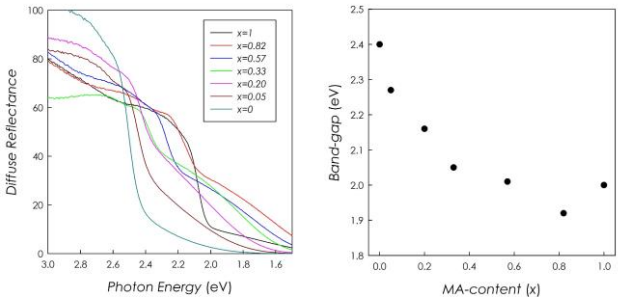

Figure 5. a) Diffuse reflectance spectra for the $FA_{1-x}MA_xSnBr_3$ solid solution; b) energy gap trend as a function of *x*.

From Figure 5 it is possible to observe a progressive decrease of the band-gap by increasing *x* up to 0.82, where an

upturn is observed for $MASnBr_3$. The E_g value for $FASnBr_3$ has not yet been measured in the current literature, but only theoretically estimated to be around 2.58 eV.[33] The present experimental value of ca. 2.40 eV is in fairly good agreement with the value calculated from the GW-BSE theory (Bethe-Salpeter equation).[33] The band-gap value for the other end-member of the solid solution, namely $MASnBr_3$, has been reported to be around 2.15 eV, in good agreement with the present value of about 2.0 eV. The small discrepancy between the two E_g values is probably due to the nature of the samples (films in ref. 33 and powders in the present paper) and to the measurement method.[34]

Starting from $FASnBr_3$, the band-gap value progressively reduces from 2.4 eV (x=0) down to ~1.92 eV (x=0.82), *i.e*. of about 0.5 eV, which is a huge energy variation for a cation replacement. Such high values are usually observed for B-cation or X-anion replacements.[3,9,35-37] This trend is in contrast with other FA/MA mixed systems, such as the $FA_{1-x}MA_xPbI_3$ solid solution, where a progressive increase of the band-gap is observed by decreasing the FA content.[6] Moreover, the complete FA/MA replacement in $FA_{1-x}MA_xPbI_3$ leads to an overall shift in the band gap of less than 0.1 eV across the whole composition range (*i.e.*, $0 \le x \le 1$). These results are quite surprising considering that the contribution of the A site cation to the density of states close to valence or conduction band edges is usually expected to be negligible, and thus the effect of cation replacement on the energy gap is indirect and related to the variation of lattice size.[6]

However, the experimental results reported here for the $FA_{1-x}MA_xSnBr_3$ solid solution, clearly show a very wide tuning of the band-gap induced by the FA/MA substitution suggesting a contribution of the A-site cation to the joint density of states in this system. As a matter of fact, our evidences are in very nice agreement with recent theoretical calculations showing that, for cubic Sn-based hybrid perovskites, the *p*-electrons of N and C atoms partially contribute to the valence band top.[38] In particular, for $FASnX_3$ perovskites the *p*-electrons of both N and C atoms give a contribution to the VBT (Valence Band Top) while for $MASnX_3$ systems only the *p*-states of N atoms partially contribute to the VBT.

With these theoretical arguments, the strong variation of the band-gap from $FASnBr_3$ up to x=0.82 in the mixed $FA_{1-x}MA_xSnBr_3$ system may result by the interplay of the N and C *p*-states contributing to the DOS and a lattice effect induced by the size difference between the two cations. When reaching the pure $MASnBr_3$ system, we are facing a different situation where C electronic states are no longer affecting the electronic structure and, looking from this side of the solid solution, already a small amount of FA cation (*i.e.*, 0.18) effectively reduces the band-gap of about 0.081 eV. The experimental results reported in this work, showing an impressive modulation of the band-gap as a function of A-site cation replacement, merit to be further investigated from a theoretical point of view, in particularly considering the role of mixed FA/MA composition in tin-based halides.

Conclusions

In the present paper we investigated the synthesis, crystal structure and optical properties of the $FA_{1-x}MA_xSnBr_3$ system, with a particular care in defining the FA/MA stoichiometries by means of NMR, and reporting for the first time the $FASnBr_3$ material. The results confirm the formation of a solid solution between the two end members, which possess a cubic symmetry with lattice parameter and cell volume obeying the Vegard's law. The investigation of the optical properties revealed an impressive and unexpected variation of the band-gap induced by the FA/MA substitution, which leads to a wide tuning of the E_g in the $FA_{1-x}MA_xSnBr_3$ system from 2.4 to 1.9 eV just by adjusting the ratio of the protonated amines. One possible origin of this new phenomenon in hybrid perovskite is the contribution of MA and/or FA to the density of states and in turn to the valence band characteristics, as indicated by theoretical calculation. If further confirmed by additional electronic structure modelling works, the $FA_{1-x}MA_xSnBr_3$ solid solution would represent the first example of an organic-inorganic hybrid perovskite system where the A-site cation has a profound impact on the electronic structure and allows an unprecedented wide tuning of optical properties by cation replacement.

Acknowledgements

The authors gratefully acknowledge the project PERSEO-"PERovskite-based Solar cells: towards high Efficiency and lOng-term stability" (Bando PRIN 2015-Italian Ministry of University and Scientific Research (MIUR) Decreto Direttoriale 4 novembre 2015 n. 2488, project number 20155LECAJ) for funding.

Notes and references

1 N.J. Jeon, J.H. Noh, W.S. Yang, Y. Kim, S. Ryu, J. Seo, S. Seok, *Nature*, 2015, **517**, 476.
2 N. Pellet, P. Gao, G. Gregori, T.-Y. Yang, M. Nazeeruddin, J. Maier, *Angew. Chem. Int. Ed.*, 2014, **53**, 3151.
3 T.J. Jacobsson, J.-P. Correa-Baena, M. Pazoki, M. Saliba, K. Schenk, M. Graetzel, A. Hagfeldt, *Energy Environ. Sci.*, 2016, **9**, 1706.
4 W.S. Yang, J.H. Noh, N.J. Jeon, Y.C. Kim, S. Ryu, J. Seo, S. Seok, *Science*, 2015, **348**, 1234.
5 Z. Yang, C.-C. Chueh, P.-W. Liang, M. Crump, F. Lin, Z. Zhu, A. K.-Y. Jen, *Nano Energy*, 2016, **22**, 328.
6 O.J. Weber, B. Charles, M.T. Weller, *J. Mater. Chem. A*, 2016, **4**, 15375.
7 A. Mancini, P. Quadrelli, G. Amoroso, C. Milanese, M. Boiocchi, A. Sironi, M. Patrini, G. Guizzetti, L. Malavasi, *J. Solid State Chem.*, 2016, **240**, 55.
8 M. Patrini, P. Quadrelli, C. Milanese, L. Malavasi, *Inorg. Chem.*, 2016, **55**, 12752.
9 A. Mancini, P. Quadrelli, C. Milanese, M. Patrini, G. Guizzetti, L. Malavasi, *Inorg. Chem.*, 2015, **54**, 8893.
10 F. Hao, C.C. Stoumpos, R.P.H. Chang, M.G. Kanatzidis, *J. Am. Chem. Soc.*, 2014, **136**, 8094.
11 C. C. Stoumpos, C.D. Malliakas, M.G. Kanatzidis, *Inorg. Chem.* 2013, **52**, 9019.

12 T. M. Koh, T. Krishnamoorthy, N. Yantara, C. Shi, W. L. Leong, P. P. Boix, A. C. Grimsdale, S. G. Mhaisalkar, N. Mathews, *J. Mater. Chem. A*, 2015, **3**, 14996.
13 M.-C.l Jung, S. R. Raga, Y. Qi, *RSC Adv*., 2016, **6**, 2819.
14 I. Borriello, G. Cantele, D. Ninno, *Phys. Rev. B: Condens. Matter Mater. Phys.* 2008, **77**, 235214.
15 E. Mosconi, P. Umari, F. de Angelis, *J. Mater. Chem*. A 2015, **3**, 9208.
16 T.-B. Song, T. Yokoyama, C. C. Stoumpos, J. Logsdon, D. H. Cao, M. R. Wasielewski, S. Aramaki, M. G. Kanatzidis, *J. Am. Chem. Soc*., 2017, **139**, 836.
17 L. Ma, F. Hao, C. C. Stoumpos, B. T. Phelan, M. R. Wasielewski, M. G. Kanatzidis, *J. Am. Chem. Soc*., 2016, **138**, 14750.
18 W. Liao, D. Zhao, Y. Yu, N. Shrestha, K. Ghimire, C. R. Grice, C. Wang, Y. Xiao, A. J. Cimaroli, R. J. Ellingson, N. J. Podraza, K. Zhu, R.-G. Xiong, Y. Yan, *J. Am. Chem. Soc*., 2016, **138**, 12360.
19 F. Hao, C. C. Stoumpos, D. H. Cao, R. P. H. Chang and M. G. Kanatzidis, *Nat. Photonics*, 2014, **8**, 489.
20 N. K. Noel, S. D. Stranks, A. Abate, C. Wehrenfennig, S. Guarnera, A.-A. Haghighirad, A. Sadhanala, G. E. Eperon, S. K. Pathak, M. B. Johnston, A. Petrozza, L. M. Herz and H. J. Snaith, *Energy Environ. Sci*., 2014, **7**, 3061.
21 M.-C. Jung, S. R. Raga, Y. Qi, *RSC Adv*., 2016, **6**, 2819.
22 T. Yokoyama, T.-B. Song, D. H. Cao, C. C. Stoumpos, S. Aramaki, M. G. Kanatzidis, *ACS Energy Lett*., 2017, **2**, 22.
23 S. J. Lee, S. S. Shin, Y. C. Kim, D. Kim, T. K. Ahn, J. H. Noh, J. Seo, S. Il Seok, *J. Am. Chem. Soc*., 2016, **138**, 3974.
24 J. Rodríguez-Carvajal, *Phys. B Condens. Matter* 1993, **192**, 55.
25 D. Massiot, F. Fayon, M. Capron, I. King, S. Le Calve, B. Alonso, J. O. Durand, B. Bujoli, Z. Gan, G. Hoatson, *Magn. Reson. Chem*., 2002, **40**, 70.
26 O. J. Weber, B. Charles and M. T. Weller, *J. Mater. Chem. A*, 2016, **4**, 15375.
27 J.-W. Lee, D.-J. Seol, A.-N. Cho, N.-G. Park, *Adv. Mater*., 2014, **26**, 4991.
28 Y. Fu, H. Zhu, A.W. Schrader, D. Liang, Q. Ding, P. Joshi, L. Hwang, X.-Y. Zhu, *Nano Lett*., 2016, **16**, 1000.
29 T. Baikie, N.S. Barrow, Y. Fang, P.J. Keenan, P.R. Slater, R.O. Piltz, M. Gutmann, S.G. Mhaisalkar, T. J. A. White, *J. Mater. Chem. A*, 2015, **3**, 9298.
30 I. Swainson, L. Chi, J.-H. Her, L. Cranswick, P. Stephens, B. Winkler, D. J. Wilson. V. Milman, *Acta Cryst. B*, 2010, **66**, 422.
31 P. Kubelka; F. Munk, *Zeit. Fur Tekn. Physik*, 1931, **12**, 593.
32 H.-S. Kim, C.R. Lee, J.-H. Im, K.-B. Lee, T. Moehl, A. Marchioro, S.-J. Moon, R. Humphry-Baker, J.-H. Yum, J. E. Moser, M. Graetzel, N.-G. Park, *Scientific Reports*, 2012, **2**, 591.
33 M. Bokdam, T. Sander, A. Stroppa, S. Picozzi, D.D. Sarma, C. Franchini, G. Kresse, *Scientific Reports*, 2016, **6**, 28618.
34 F. Hao, C.C. Stoumpos, D.H. Cao, R.P. Chang, M.G. Kanatzidis, *Nat. Photonics*, 2014, **8**, 489.
35 F. Brivio, K. T. Butler, A. Walsh and M. Van Schilfgaarde, *Phys. Rev. B: Condens. Matter Mater. Phys.*, 2014, **89**, 155204.
36 I. Borriello, G. Cantele and D. Ninno, *Phys. Rev. B: Condens. Matter Mater*., 2008, **77**, 235214.
37 T. Umebayashi, K. Asai, T. Kondo and A. Nakao, *Phys. Rev. B: Condens. Matter Mater. Phys*., 2003, **67**, 155405.
38 Z.-Q. Ma, H. Pan, P. K. Wong, *J. Electron. Mater*., 2016, **45**, 5956.